

Ethylene Detection Using Nanoporous PtTiO₂ Coatings Applied to Magnetoelastic Thick Films

Rhong Zhang¹, M. I. Tejedor¹, Marc A. Anderson^{1,*}, Maggie Paulose² and Craig A. Grimes²

¹ Environmental Chemistry & Technology Program, University of Wisconsin-Madison, Madison, WI

² Department of Electrical Engineering & Materials Research Institute, 217 Materials Research Laboratory, The Pennsylvania State University, University Park, PA 16802

* Author to whom correspondence should be addressed. E-mail: nanopor@facstaff.wisc.edu

Received: 25 June 2002 / Accepted: 26 June 2002 / Published: 22 August 2002

Abstract: This paper reports on the use of nanoporous Pt-TiO₂ thin films coated onto magnetoelastic sensors for the detection of ethylene, an important plant growth hormone. Five different metal oxide coatings, TiO₂, TiO₂+ZrO₂, TiO₂+TTCN(1,4,7-Trithiacyclononane)+Ag, SiO₂+Fe, and TiO₂+Pt, each having demonstrated photocatalytic activity in response to ethylene, were investigated for their ability to change mass or elasticity in response to changing ethylene concentration. Pt-TiO₂ films were found to possess the highest sensitivities, and coupled with the magnetoelastic sensor platform capable of sensing ethylene levels of < 1 ppm.

Key words: Ethylene, Sensor, Metal Oxide, Magnetoelastic, Nanoporous

Introduction

Ethylene is a plant hormone used in the regulation of metabolic processes vital in both fruit ripening and leaf-abscission. For example, ethylene has been found to induce, or be correlated with, the ripening of cantaloupe [1,2], apples [3] and tomatoes [4]. Ethylene levels have also been correlated with increasing plant respiration [5]. Traditionally gas chromatographic systems (GC) [6, 7] and photoacoustic detection systems [8] have been used to measure ethylene. However such instruments are generally impractical for in-situ real-time measurements, requiring gas samples to be measured only after returning to the laboratory. Therefore in-situ ethylene sensors of high-sensitivity are of great interest. As described herein we use nanoporous PtTiO₂ films, the mass/elasticity of which respond to

ethylene concentrations, with magnetoelastic sensors [9-16] to measure ethylene at low concentrations (< 1 ppm).

As illustrated in Figure 1, in response to a time varying magnetic-field magnetoelastic thick-film sensors vibrate at a characteristic resonant frequency. Tracking changes in the resonant frequency of an uncoated (bare) magnetoelastic sensor enables measurement of fluid flow velocity [9], pressure [11], temperature [13], and liquid density and viscosity [13].

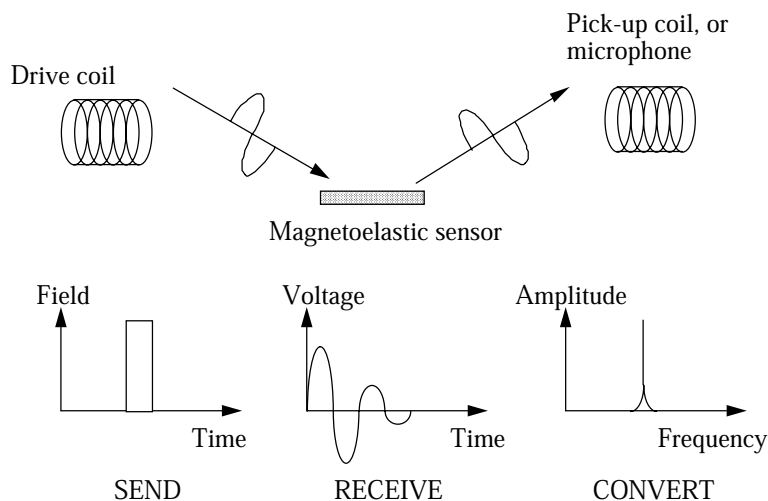


Figure 1. Drawing illustrating the remote query nature of magnetoelastic sensors. A magnetic field impulse is applied to the sensor; the transient response is captured using either a pickup coil to detect the magnetic flux or a microphone to detect the mechanical vibrations, and then converted into the frequency domain using a fast Fourier transform. The resonant frequency is tracked to provide chemical and environmental information.

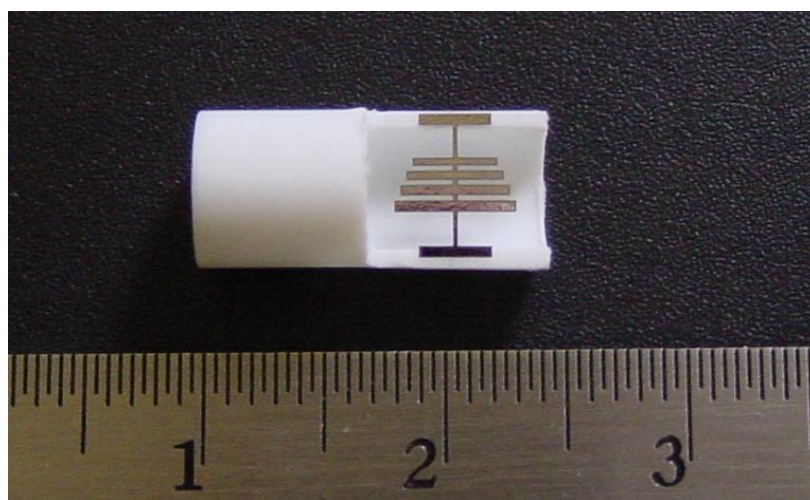


Figure 2. A four-element magnetoelastic sensor array mounted in an air-flow tube. The sensor array was fabricated from a continuous ribbon using a computer controlled laser-cutting tool. The major scale of the ruler is in centimeter.

The resonant frequency of a magnetoelastic sensor changes with application of a small mass load, and elasticity of the applied mass load [15,16]. Hence application of an analyte responsive

mass/elasticity changing layer to a magnetoelastic substrate enables fabrication of a highly sensitive, compact, and inexpensive chemical sensor platform. Compared with surface acoustic wave devices magnetoelastic sensors are approximately 10^4 cheaper enabling their use on a disposable basis, approximately ten times smaller (see Figure 2) enabling more information to be obtained per given sensing area, and of comparable sensitivity. The magnetoelastic sensors used in this work, laser-cut from a continuous 28 μm thick ribbon purchased commercially from Honeywell Corporation (alloy 2826MB), are composition $\text{Fe}_{40}\text{Ni}_{40}\text{P}_{14}\text{B}_6$.

The fundamental resonant frequency f_r of a ribbon-like sensor of width W , thickness T_s , length L , Young's modulus Y and density ρ is given by [16]:

$$f_r = \sqrt{\frac{Y}{\rho}} \cdot \frac{1}{2L} \quad (1)$$

If a magnetoelastic sensor is coated with a layer of elastic material in which the speed of sound is not the same as in the sensor material the resonant frequency will change. A negative frequency shift Δf in response to a mass load Δm was derived earlier as [13]

$$\Delta f = -f_0 \frac{\Delta m}{2m_0} \quad (2)$$

where f_0 is the initial resonant frequency and m_0 is the initial mass of the sensor. However Eq. 2 does not account for elastic stress in the applied mass load, and is only valid if the applied mass load is subject to an oscillating translational motion, rather than an oscillating contraction and expansion. If the coating is thick compared to the surface roughness the effect of the coating elasticity prevails.

Under application of a force, for thin coatings the coating and the sensor material have a common tensile strain ε . Letting F_{tot} represent the superposition of the tensile force in the coating F_c and in the sensor F_s and $\varepsilon = \varepsilon_c = \varepsilon_s$, we can calculate the effective Young's Modulus of elasticity of the sensor-coating compound as

$$Y_{eff} = \alpha_c \cdot Y_c + \alpha_s \cdot Y_s \quad (3)$$

where α_c and α_s are the fractional cross section ($A/A_{total} = \alpha$) of the coating and sensor respectively. The effective density of a coated sensor is given when relating the total mass $m' = m_c + m_0$ to the separate masses of coating m_c and sensor m_0 resulting in

$$\rho_{eff} = \alpha_c \cdot \rho_c + \alpha_s \cdot \rho_s \quad (4)$$

We define the sound velocity of an uncoated sensor as

$$v_0 = \sqrt{Y_s / \rho_s} \quad (5)$$

and the sound velocity of a coated sensor as

$$v' = \sqrt{Y_{eff} / \rho_{eff}} \quad (6)$$

The ratio of the sound velocities before and after a coating is applied can be written as

$$\frac{v'}{v_0} = \sqrt{\frac{\alpha_c \cdot Y_c + \alpha_s \cdot Y_s}{\alpha_c \cdot \rho_c + \alpha_s \cdot \rho_s}} \cdot \sqrt{\frac{\rho_s}{Y_s}} = \sqrt{\frac{1 + \alpha_c \cdot (Y_c/Y_s - 1)}{1 + \alpha_c \cdot (\rho_c/\rho_s - 1)}} \quad (7)$$

The same expression written in terms of the applied mass load yields

$$\frac{v'}{v_0} = \sqrt{(1 - \beta^2) \frac{m_0}{m'} + \beta^2} = \sqrt{\frac{m_0}{m'} + \beta^2 \left(1 - \frac{m_0}{m'}\right)} \quad (8)$$

with β being the parameter determining the slope and sign of the frequency change upon an applied coating and

$$\beta = \frac{\sqrt{Y_c/\rho_c}}{\sqrt{Y_s/\rho_s}} = \frac{v_c}{v_0} \quad (9)$$

The sensitivity, defined as the change of the resonant frequency due to an applied coating, depends upon ratio β , the sound velocity in the coating to that in the sensor; if β is close to one the resonant frequency would not change.

Experimental Methods

The gas sensor is comprised of three layers: the magnetoelastic substrate, a sputtered ≈ 20 nm Pt layer used to promote adhesion, deposited on each side of the sensor, and the ethylene responsive nanoporous oxide layer deposited via sol gel per dip coating. The dimensions of the sensors used in this work were 40 mm in length, 5 mm in width, and 28 μm in thickness. Per Eq. 1, the length of the sensor determines the nominal operating frequency range of the sensor; a 40 mm long sensor has a resonant frequency of approximately 59 kHz. We are able to measure sensor response to an accuracy of approximately 1 Hz. Figure 3 shows the measurement apparatus; the sensor under test is placed within the white cylinder, located between the two coils on the right, through which the test gas of interest is passed. A computer controlled signal generator is used to generate the excitation signal, which is then amplified to expose the sensor to a time varying magnetic field of 50 mOe intensity. The sensor is exposed to a d.c. magnetic biasing field of approximately 4 Oe, used to overcome the anisotropy field of the sensor optimizing its performance, by adjacent location of a magnetically hard thick film. The output from the pickup coil used to monitor the sensor is fed into a lock-in amplifier, with the output fed into a computer used to control the measurement and operation.

The thin-film nanoporous oxides investigated were prepared by sol-gel methods [18-20], with the magnetoelastic sensors, after sputter-coating the sensors with the adhesion promoting Pt layer, dip-coated in the sol and withdrawn at a rate of 0.95 mm/s; the average pore size of TiO_2 thin films was approximately 7.7 nm [21]. The films were dried and subsequently fired at 300°C to achieve thin films comprised of 10 nm particles, with an average porosity of 35% and specific surface area of 160 m^2/g . Figure 4 shows the porosity and surface area of the Pt- TiO_2 films as a function of firing temperature.

We investigated TiO_2 , $\text{TiO}_2+\text{ZrO}_2$ (TiO_2 88%, ZrO_2 12%); TiO_2+TTCN (1,4,7-Trithiacyclononane)+Ag (TiO_2 96%, TTCN 2%, Ag 2%); SiO_2+Fe (SiO_2 82%, Fe 18%); and $\text{TiO}_2\text{-Pt}$ (TiO_2 94%, Pt 6%) thin films for a mass/elasticity changing response to ethylene; earlier work [22] has shown the ethylene dependent photo-catalytic activity of such materials. The thickness of each layer applied to the sensor was 31 ± 1 nm, we investigated the response of magnetoelastic sensors coated with one to five applied layers, with corresponding thicknesses of 31, 62, 93, and 155 nm. All of the experimental tests were conducted at room temperature of approximately 19°C. A mass flow

controller was used to control the ethylene gas flow through a sensor-containing test chamber; a pickup coil wrapped around the 5 cm diameter test chamber was used to monitor the sensor.



Figure 3. The magnetoelastic sensor system. A signal generator sends a pulse-like excitation signal, appropriately amplified, to the interrogation coils. The response of the sensor, located in the white tube placed between the two coils, is monitored with a pickup coil the output of which is passed to a lock-in amplifier. A computer controls the instrumentation and plots measured parameters as a function of time.

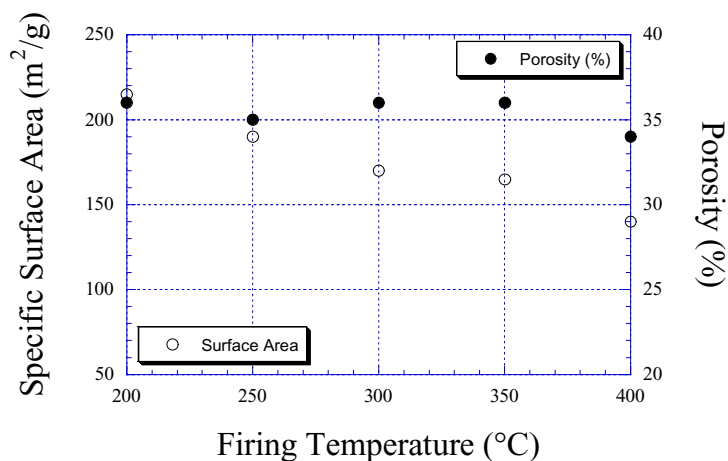


Figure 4. Effect of firing temperature on the porosity and surface area of Pt-TiO₂ films.

Experimental Results

Our initial studies of the different metal oxide thin films showed that the Pt-TiO₂ films have the greatest sensitivity to ethylene, at least a factor of 2.5 over the other metal oxides investigated, and hence this composition was used in all reported studies. Changing the thickness of the metal oxide layer alters the behavior of the sensor; while a thicker analyte response layer offers a greater swing in sensor mass load, and thereby a corresponding greater shift in resonant frequency, increasing mass loads reduce the ability of the sensor to oscillate thereby reducing the quality factor of the sensor and

hence the accuracy at which the resonant frequency can be determined, and also slows the response time of the sensors due to rate limits imposed by diffusion. Hence an optimal coating thickness needs to be determined as a function of the relative difference between the speed of sound in the sensor and coating material, as well as the desired response time.

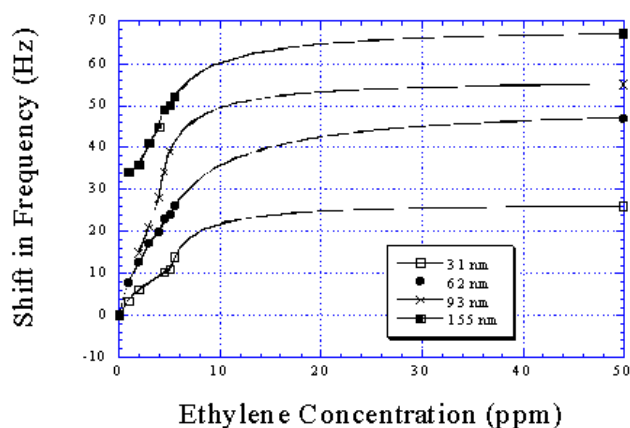


Figure 5. Shift in measured resonant frequency of ethylene sensors, of variable Pt-TiO₂ coating thickness approximately, as a function of ethylene concentration. Measurements were taken at 19°C.

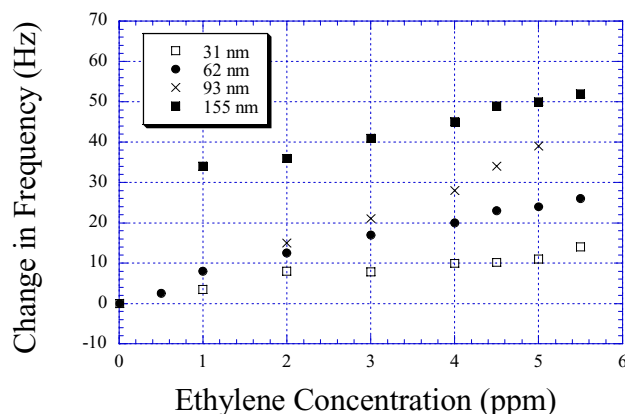


Figure 6. Shift in measured resonant frequency of ethylene sensors at low ppm levels.

Ethylene sensors, comprised of magnetoelastic sensors having Pt-TiO₂ coatings of \approx 31, 62, 93, and 155 nm (both sides) were tested for their ability to detect ethylene. Figure 5 shows the absolute change in measured resonant frequency as a function of ethylene concentration (ethylene mixed with dry nitrogen to achieve desired ethylene concentration) and Pt-TiO₂ coating thickness; the resonant frequency of the sensor shifts downward with increasing ethylene concentration. The target gas mixture was flowed over the sensor for ten minutes prior to measurement to ensure a steady state response. The response saturates after reaching an ethylene concentration of approximately 100 ppm. The measured frequency response follows a Langmuir model, $KbC/(1 + KC)$, where C = concentration with model parameters K and b selected to give the best fit to the data; for the 31 nm thick coating $k =$

0.16, $b = 30$. Figure 6 shows the response of the ethylene sensors as a function of PtTiO₂ coating thickness expanded to more clearly delineate the response at low ppm levels.

It is well known that metal oxide films are excellent absorbers of moisture. Hence a key issue to the successful use of PtTiO₂ films for monitoring ethylene is the ability to compensate for the effect of humidity on sensor performance. For example, while the 155 nm coated sensor had a 65 Hz change in the measured resonant frequency from dry nitrogen to a 50 ppm ethylene mixture, the same sensor had a frequency shift of 500 Hz going between dry nitrogen and nitrogen with a 25% relative humidity. Compensation for the effect of humidity on ethylene measurements by the PtTiO₂ films could be accomplished using magnetoelastic sensors coated with SiO₂+Fe (SiO₂ 82%, Fe 18%), a composition found to have no measurable response to ethylene but a humidity response virtually identical to that of the PtTiO₂ films; cross-correlation [23] between the two sensors would enable ethylene measurement independent of humidity.

Conclusions

Thin films composed of nanoporous PtTiO₂ have been used to detect low concentrations of ethylene (< 1 ppm), an analyte important for characterizing plant growth. The change in resonant frequency of the PtTiO₂ coated magnetoelastic sensors in response to variable ethylene concentrations can be modeled with a Langmuir equation. Thicker PtTiO₂ films resulted in larger frequency shifts but had longer response times. At low concentrations the resonant frequency of the sensor shifted linearly with ethylene concentration. Future work will focus on the ability of this sensor platform to monitor \approx ppb levels of ethylene.

Acknowledgements

The authors gratefully acknowledge support of this work by the National Science Foundation through grant ECS-0196494.

References

1. Kendall, S.A.; Ng, T.J. Genetic-variation of Ethylene Production in Harvested Muskmelon Fruits. *Hort. Science* **1988**, *28*, 759-761.
2. Lacan, D.; Baccou, J.C. Changes in Lipids and Electrolyte Leakage During Non-netted Muskmelon Ripening. *J Amer Soc Hort Sci* **1996**, *121*(3), 554-558.
3. Gussman, C.D.; Goffreda, J.C.; Gianfagna, T.J. Ethylene Production and Fruit-softening rates in Several Apple Fruit Ripening Variants. *Hort. Science* **1993**, *28*, 135-137.
4. Güçlü, J; Paulin, A.; Soudain, P. Changes in Polar Lipids during ripening and senescence of cherry Tomato (*Lycopersicon-esculentum*) - relation to Climacteric and Ethylene Increases. *Physiol. Plant* **1989**, *77*, 413-419.
5. Brady, C. J. Fruit Ripening. Review of Plant Physiology. *Plant Molecular Biology* **1987**, *38*, 155-178.

6. Pham-Tuan, H.; Vercammen, J.; Davos, C. Automated Capillary Gas Chromatographic System to Monitor Ethylene Emitted from Biological Materials. *J. Chromatography A* **2000**, *868*(2), 249-259.
7. Eklund, L.; Little, C.H.A. Ethylene Evolution, Radial Growth and Carbohydrate Concentrations in *Abies Balsamea* Shoots Ringed with Ethrel. *Tree Physiology* **1998**, *18*(6), 383-391.
8. De Vries, H.S.M.; Wasono, M.A.J.; Harren, F.J.M. Ethylene and CO₂ Emission Rates and Pathways in Harvested Fruits Investigated, In-situ, by Laser Photothermal Deflection and Photoacoustic Techniques. *Postarvest Biol Tec* **1996**, *8*(1), 1-10.
9. Grimes, C.A.; Kouzoudis, D. Remote Query Measurement of Pressure, Fluid-Flow Velocity, and Humidity Using Magnetoelastic Thick-Film Sensors. *Sensors and Actuators* **2000**, *84*, 205-212.
10. Cai, Q.Y.; Cammers, A.; Grimes, C. A. A Wireless, Remote Query Magnetoelastic CO₂ Sensor. *Journal of Environmental Monitoring* **2000**, *2*, 556-560.
11. Kouzoudis, D.; Grimes, C. A. The Frequency Response of Magnetoelastic Sensors to Stress and Atmospheric Pressure. *Smart Materials and Structures* **2000**, *9*, 1-5.
12. Grimes, C.A.; Kouzoudis, D.; Dickey, E. C.; Qian, E. C.; Anderson, M. A.; Shahidain, R.; Lindsey, M.; Green, L. Magnetoelastic Sensors in Combination With Nanometer-Scale Honeycombed Thin Film Ceramic TiO₂ For Remote Query Measurement Of Humidity, *Journal of Applied Physics* **2000**, *87*(9), 5341-5343.
13. Grimes, C.A.; Ong, K. G.; Loisel, K.; Stoyanov, P. G.; Kouzoudis, D.; Liu, Y.; Tong, C. Magnetoelastic Sensors For Remote Query Environmental Monitoring. *Smart Materials and Structures* **1999**, *8*, 639-646.
14. Cai, Q.; Jain, M.K.; Grimes, C.A. A wireless, remote query ammonia sensor. *Sensors and Actuators B* **2001**, *77*, 614-619.
15. Schmidt, S.; Grimes, C.A. Elastic modulus measurement of thin films coated on magnetoelastic ribbons. *IEEE. Trans. on Magnetics* **2001**, *37*(4), 2731-2733.
16. Schmidt, S.; Grimes, C.A. Characterization of nano-dimensional thin-film elastic moduli using magnetoelastic sensors. *Sensors and Actuators A* **2001**, *94*, 189-196.
17. See product information at <http://www.vacuumschmelze.de>.
18. Xu, Q.; Anderson, M.A. Sol-gel route to synthesis of microporous ceramic membranes: thermal stability of TiO₂-ZrO₂ mixed oxide. *J. Am. Ceram. Soc.* **1993**, *76*(8), 2093-2097.
19. Chu, L.; Tejedor-Tejedor, M.; Anderson, M. A. Particulate sol-gel route for microporous silica gel. *Microporous Materials* **1997**, *8*, 207-213.
20. Peterson, ; Anderson, M. A.; Hill, C.G. Development of TiO₂ membranes for gas phase manofiltration. *J. of Membrane Science* **1994**, *94*, 103-109.
21. Vichi, F. M.; Colomer, M. T.; Anderson, M.A. Nanopore ceramic membranes as novel electrolytes for proton exchange membranes. *Electrochemical and Solid-State Letters* **1999**, *2*(7), 313-316.
22. Zorn, M. E.; Tompkins, D. T.; Zeltner, W. A.; Anderson, M. A. Catalytic and photocatalytic Oxidation of ethylene on Titania-based thin-films. *Environ. Sci. technol.* **2000**, *34*, 5206-5210.
23. Cai, Q.; Grimes, C. A. A Salt Independent pH Sensor. *Sensors and Actuators B* **2001**, *79*, 144-149.

Sample Availability: Available from the authors.